

# Oxidative dehydrogenation of ethanol over Cu/Mg-Al catalyst derived from hydrotalcite: effect of ethanol concentration and reduction conditions\*

Piriya PINTHONG, Piyasan PRASERTHDAM, Bunjerd JONGSOMJIT<sup>†‡</sup>

*Center of Excellence on Catalysis and Catalytic Reaction Engineering, Department of Chemical Engineering,  
Faculty of Engineering, Chulalongkorn University, Bangkok 10330, Thailand*

<sup>†</sup>E-mail: bunjerd.j@chula.ac.th

Received Sept. 7, 2019; Revision accepted Jan. 9, 2020; Crosschecked Feb. 19, 2020

**Abstract:** The copper-modified Mg-Al catalyst (Cu/Mg-Al) was synthesized using the incipient wetness impregnation of copper onto the Mg-Al hydrotalcite derived from co-precipitation method. The effects of copper on the characteristics of catalyst were obtained using several characterization techniques. We found that only copper (I) oxide (CuO) species were obtained on the surface after calcination in air by X-ray Diffraction (XRD). However, the basicity of the base decreases slightly, while the density of the base increases due to the decrease in Brunauer-Emmett-Teller (BET) surface area. We carried out the catalytic activity of the Cu/Mg-Al catalyst in the continuous flow reactor through oxidative dehydrogenation of ethanol. We obtained that the copper enhances the catalytic activity in this reaction, and the ethanol conversion increases with increase in temperature, while the acetaldehyde selectivity decreases because of the decomposition of acetaldehyde to carbon dioxide. The highest acetaldehyde yield of 41.8% was at 350 °C. Moreover, we studied the effects of the ethanol concentration by varying the ethanol feed concentrations (99.9%, 75%, and 50%). The ethanol conversion decreases with a decrease in the ethanol concentration due to the high adsorption of water molecules on the catalyst surface. Thus, the negative effect decreases at higher reaction temperature (350–400 °C). Furthermore, we investigated the effect of the reduction condition of catalyst by varying the reduction temperature (300 and 400 °C). The reduction process affects the catalytic activity. The Cu/Mg-Al was comparatively stable for 10 h upon time-on-stream test. It is used as a promising catalyst in oxidative dehydrogenation of ethanol without any reduction step.

**Key words:** Oxidative dehydrogenation; Ethanol; Copper; Mg-Al hydrotalcite; Acetaldehyde; Catalyst  
<https://doi.org/10.1631/jzus.A1900451>

**CLC number:** O622

## 1 Introduction

Recently, several emphases have been made on an alternative renewable energy due to the problems of using fossil-based resources. In particular, the

production of bioenergy from agricultural waste has been of great interest, especially for vehicles. Bioethanol is one of the alternative fuels obtained from biomass resources such as sugarcane, cassava, algae, and even agricultural waste (Papong and Malakul, 2010; Dias et al., 2011; Kumar et al., 2013). In several industries such as the production of ethyl acetate and acetic acid, the acetaldehyde has been used extensively (Mallat and Baiker, 2004; Shan et al., 2017). Moreover, bioethanol is used as a raw material for the acetaldehyde production through the oxidative dehydrogenation reaction over suitable catalysts (Gomez et al., 1997; Quaranta et al., 1997; Tu and Chen,

<sup>‡</sup> Corresponding author

\* Project supported by Chulalongkorn University and the Thailand Science Research and Innovation (TSRI) under Catalytic Reaction (CAT-REAC) Industrial Project

 ORCID: Piriya PINTHONG, <https://orcid.org/0000-0002-1061-0780>; Bunjerd JONGSOMJIT, <https://orcid.org/0000-0002-9558-9190>

© Zhejiang University and Springer-Verlag GmbH Germany, part of Springer Nature 2020

2001). However, research shows that the oxidative dehydrogenation reaction is preferred over non-oxidative dehydrogenation because it requires lower reaction temperature to prevent coking and metal sintering problems (Liu et al., 2017).

Furthermore, a structure of hydrotalcite is brucite-like and contains Mg atoms substituted with Al atoms leading to give positive charge layer and anionic layer in the interlayer (Yang et al., 2002). We observe that the calcination of the hydrotalcite produces the basic mixed oxide through dehydroxylation. Moreover, the major property of this material is the basicity of the surface, which promotes the abstraction of protons from hydrocarbon in dehydrogenation reaction (Sikander et al., 2017). In our previous study (Pinthong et al., 2019), we examined the mixed oxide obtained from the calcination of hydrotalcite using the oxidative dehydrogenation of ethanol; however, the catalytic result seems to be fairly low. Hence, to promote the catalytic activity, the modification of mixed oxide is crucial. Several studies show that the copper-containing catalysts is responsible for the high active catalysts in various reactions such as phenol alkylation (Velu and Swamy, 1996a, 1996b), selective conversion of ethanol (Hosoglu et al., 2015), and oxidation of ketone (Kaneda et al., 1995). Furthermore, the modification of the activated carbon catalyst by loading copper on the surface shows a positive effect in the dehydrogenation of ethanol to acetaldehyde (Ob-eye et al., 2019). However, using a fermentation process, the production of bioethanol leads to the formation of water in the ethanol solution. Therefore, we need to clarify the effect of the ethanol concentrations. Hence, Wu et al. (2013) and Krutpijit and Jongsomjit (2017) carried an investigation on this effect on the catalytic activity.

In this study, we investigated the effect of copper on the catalytic activity of Mg-Al oxide obtained from the hydrotalcite. To achieve this, we prepared the copper-modified catalyst (Cu/Mg-Al) characterized by the X-ray Diffraction (XRD), nitrogen adsorption, temperature-programmed desorption of carbon dioxide (CO<sub>2</sub>-TPD), and temperature-programmed reduction by hydrogen (H<sub>2</sub>-TPR) techniques. We investigated the catalytic behaviors using the oxidative dehydrogenation of ethanol to acetaldehyde at specific conditions. Furthermore, we used ethanol with different concentrations to study the effect of

water on the catalytic activity. Also, we examined the effect of reduction condition using pre-reducing catalyst at different temperatures before the reaction.

## 2 Experimental

### 2.1 Materials and chemicals

In this study, we synthesized the Mg-Al hydrotalcite from magnesium nitrate hexahydrate (Mg(NO<sub>3</sub>)<sub>2</sub>·6H<sub>2</sub>O), aluminum nitrate nonahydrate (Al(NO<sub>3</sub>)<sub>3</sub>·9H<sub>2</sub>O), sodium carbonate (Na<sub>2</sub>CO<sub>3</sub>), and sodium hydroxide (NaOH) purchased from Sigma-Aldrich. The metal precursor was copper (II) nitrate hemi(pentahydrate) (Cu(NO<sub>3</sub>)<sub>2</sub>·2.5H<sub>2</sub>O) purchased from Sigma-Aldrich. We used the absolute ethanol (99.9%) purchased from Merck as the reactant in the catalytic activity test. To obtain ethanol concentration of 75% and 50%, we prepared the diluted ethanol solution by mixing the absolute ethanol (99.9%) with deionized water.

### 2.2 Catalyst preparation

We synthesized the Mg-Al hydrotalcite sample using the co-precipitation method following the previous procedure (Pinthong et al., 2019). To produce Mg-Al mixed oxide (Mg-Al), the obtained Mg-Al hydrotalcite was calcined in air for 6 h at 450 °C. Furthermore, we used the incipient wetness impregnation method to prepare the copper-modified hydrotalcite catalyst (Cu/Mg-Al). Then, we dropped the aqueous solution of copper (II) nitrate into the Mg-Al mixed oxide sample to obtain the final catalyst with 5% (in weight) of Cu. Finally, it was dried at 110 °C overnight in the oven and calcined at 450 °C in air for 6 h.

### 2.3 Catalyst characterization

We analyzed the crystalline structure of the catalyst sample using a SIEMENS D 5000 XRD (Siemens, Germany) with CuK<sub>α</sub> radiation source,  $\lambda = 0.154439$  nm and Ni-filtered in the  $2\theta$  range of 10°–80°.

The specific surface area, pore-volume, and pore size diameter of catalyst were measured using a Micromeritics ASAP 2000 automated system (Micromeritics Instrument Corp., USA). The dissolved gas was removed from the catalyst sample (0.1 g) at

200 °C for 4 h before the nitrogen physisorption process at −196 °C. The specific surface area of the catalyst was measured using the Brunauer-Emmett-Teller (BET) theory. We determined the pore volume and pore size diameter using the Barrett-Joiner-Halenda (BJH) method.

To determine the basicity of catalyst, we used a CO<sub>2</sub>-TPD. The analysis was carried out using a Micromeritics Chemisorb 2750 automated system (Micromeritics Instrument Corp., USA). The catalyst sample (50 mg) was preheated using the helium flow rate of 25 cm<sup>3</sup>/min for 1 h at 450 °C, and then it was cooled to 40 °C and saturated with carbon dioxide for 30 min. The physisorbed carbon dioxide was removed using the helium flow rate of 25 cm<sup>3</sup>/min for 2 h before the temperature-programmed analysis. Moreover, we carried out the temperature-programmed desorption from 40 to 450 °C under the helium flow rate of 25 cm<sup>3</sup>/min at the heating rate of 10 °C/min. Thereafter, we analyzed the carbon dioxide desorption signal using a thermal conductivity detector. We calibrated the amount of carbon dioxide by direct pulsing with 1 mL of 10% carbon dioxide in the helium using a 6-port valve. Thus, we obtained the calibration factor by integrating the carbon dioxide pulse profile area and equating it to moles of the carbon dioxide. Hence, we determined the basicity of catalyst from the area under the peak in the CO<sub>2</sub>-TPD profile.

We investigated the reduction behavior of the catalyst using a H<sub>2</sub>-TPR. The sample pretreatment process was carried out using a similar procedure of CO<sub>2</sub>-TPD analysis. Moreover, we carried out the analysis from 40 to 550 °C at the heating rate of 10 °C/min under 10% of the hydrogen in argon. Then, we obtained a reduction profile from thermal conductivity detector.

The bulk copper content in the catalyst was measured using an Inductively Coupled Plasma-Optical Emission Spectroscopy (ICP-OES), Optima 2100 DV (PerkinElmer Inc., USA).

To determine the carbon deposition on the catalyst surface, we analyzed the spent catalyst obtained from the stability test and fresh catalyst in the thermogravimetric analyzer (STD Q600, TA Instruments, USA). The analysis was carried from 30 to 1000 °C under an oxidative atmosphere at a heating rate of 10 °C/min.

## 2.4 Reaction test

We obtained the catalytic performance of the Cu/Mg-Al catalyst through oxidative dehydrogenation of the ethanol using the previous procedure (Pinthong et al., 2019). To achieve this, we first packed the quartz wool (20 mg) and Cu/Mg-Al catalyst (50 mg) in the glass tube reactor with inner diameter of 7 mm and placed in the electric furnace. To remove moisture before the reaction test, we pre-treated the catalyst under inert atmosphere (nitrogen) at 200 °C for 30 min. During the reduction effect, Cu/Mg-Al catalyst was reduced in the hydrogen atmosphere at 300 and 400 °C for 1 h before the reaction. The ethanol with different concentrations (99.9%, 75%, and 50%) was supplied to the vaporizer using the syringe pump at the flow rate of 1.45 cm<sup>3</sup>/h and vaporized at 150 °C. The ethanol vapor was mixed with air and nitrogen gas at the flow rate of 60 cm<sup>3</sup>/min (the ethanol/oxygen/nitrogen ratio is 7.7%/22.2%/70% by volume) with a weight hourly space velocity of 22.9 h<sup>−1</sup>. Furthermore, we carried out the oxidative dehydrogenation of ethanol from 200 to 400 °C. The reaction was kept for 30 min to reach a steady-state for each temperature. Consequently, the effluent gas was analyzed using a gas chromatograph. Moreover, the hydrocarbon products were measured using a flame ionization detector, whereas CO<sub>x</sub> was analyzed using a thermal conductivity detector. Hence, we calculated the ethanol conversion ( $X_{\text{ethanol}}$ ), product selectivity ( $S_i$ ), and yield ( $Y_i$ ) using the following equations:

$$X_{\text{ethanol}} = \frac{n_{\text{ethanol}(\text{in})} - n_{\text{ethanol}(\text{out})}}{n_{\text{ethanol}(\text{in})}} \times 100\%, \quad (1)$$

$$S_i = \frac{n_i}{\sum n_i} \times 100\%, \quad (2)$$

$$Y_i = \frac{X_{\text{ethanol}} \times S_i}{100}, \quad (3)$$

where  $n_{\text{ethanol}(\text{in})}$  is the number of moles of ethanol in feed,  $n_{\text{ethanol}(\text{out})}$  is the number of moles of unreacted ethanol, and  $n_i$  is the number of moles of each product.

### 3 Results and discussion

#### 3.1 Characterization

In this study, we characterized the copper-modified Mg-Al catalyst (Cu/Mg-Al) using the XRD, nitrogen adsorption, CO<sub>2</sub>-TPD, and H<sub>2</sub>-TPR techniques and they were compared with Mg-Al mixed oxide catalyst obtained from our previous study (Pinthong et al., 2019).

The XRD results of Cu/Mg-Al catalyst (Fig. 1) show the characteristic peaks at  $2\theta \approx 43^\circ$  and  $63^\circ$ . It is assigned to MgO periclase (Aramendía et al., 1999; Ramasamy et al., 2016) and peaks at  $2\theta \approx 35.5^\circ$  and  $38.8^\circ$  showing the presence of the crystalline CuO on the catalyst surface (Li et al., 2011).

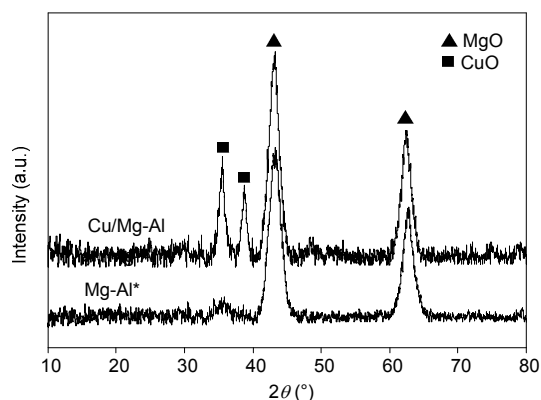


**Fig. 1** XRD patterns of catalysts

\* Values are obtained from previous work (Pinthong et al., 2019)

Here, we measured the surface area, pore volume, and pore size diameter of the catalyst using the nitrogen physisorption and the results are shown in Table 1. The specific surface area and pore volume of the Cu/Mg-Al decrease while the pore size diameter increases for the Mg-Al catalyst. Thus, the result shows the blockage of the smaller pores using CuO particles on the Mg-Al catalyst surface. Furthermore, it can be confirmed by the slight broadening of the pore size distribution of Cu/Mg-Al compared with Mg-Al catalyst (Fig. 2). Fig. 2 shows the nitrogen adsorption-desorption isotherm and pore size distribution. However, we observed the type IV isotherm with hysteresis loops in both catalysts as shown in most mesoporous materials. Also, the obtained pore size distribution shows that the pore sizes were in the range of 2–50 nm assigned to mesoporous

materials (Leofanti et al., 1998). The result agrees with the adsorption-desorption isotherm.

**Table 1** Characterization results of the catalysts

Parameter	Value	
	Mg-Al*	Cu/Mg-Al
Copper loading (% in weight)	–	4.25**
Surface area (m <sup>2</sup> /g)	168	47
Pore volume (cm <sup>3</sup> /g)	0.60	0.29
Pore size diameter (nm)	12	21
Basicity (μmol CO <sub>2</sub> /g)	253.5	251.8
Base density (μmol CO <sub>2</sub> /m <sup>2</sup> )	1.51	5.36

\* Values of Mg-Al catalyst are obtained from the previous work (Pinthong et al., 2019); \*\* Obtained from an ICP-OES

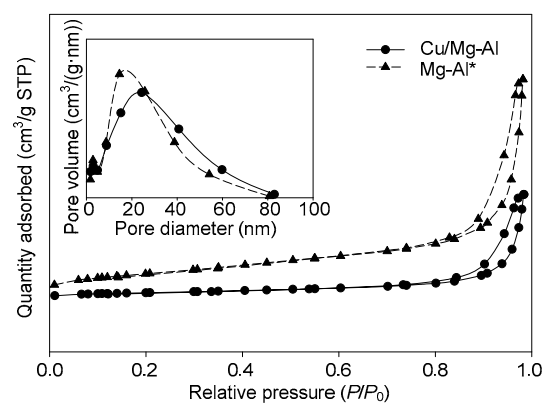


**Fig. 2** Nitrogen adsorption-desorption isotherms and pore size distributions of catalysts

\* Values are obtained from the previous work (Pinthong et al., 2019)

To determine the basicity of the catalyst, we carried out the temperature-programmed desorption of the carbon dioxide, which involved the catalytic performance of the dehydrogenation and oxidative dehydrogenation of ethanol (Dai et al., 2004; Nair et al., 2011; Blokhina et al., 2012). Fig. 3 shows the CO<sub>2</sub>-TPD profiles while the values of their basicity are shown in Table 1. The total basicity of Cu/Mg-Al catalyst (251.8 μmol CO<sub>2</sub>/g) was slightly lower than that of the Mg-Al (253.5 μmol CO<sub>2</sub>/g). Consequently, we obtained that the presence of copper in the Mg-Al mixed oxide resulted in a slight decrease in the amount of the basic site on the catalyst surface. Dixit et al. (2013) and Quesada et al. (2018) also noticed this behavior. However, the base density of the Cu/Mg-Al (5.36 μmol CO<sub>2</sub>/m<sup>2</sup>) was remarkably higher than that of the Mg-Al catalyst

( $1.51 \mu\text{mol CO}_2/\text{m}^2$ ). This is because the surface area of the Cu/Mg-Al is lower than that of the Mg-Al.

$\text{H}_2$ -TPR was used to determine the reducibility of the Cu/Mg-Al catalyst. In Fig. 4, the  $\text{H}_2$ -TPR profile shows that the reducibility of the surface copper species occurs in two steps at the maximum temperature ( $T_{\text{max}}$ ) of about  $205^\circ\text{C}$  and  $370^\circ\text{C}$  corresponding to the reduction of  $\text{CuO}$  to  $\text{Cu}_2\text{O}$  and  $\text{Cu}_2\text{O}$  to  $\text{Cu}^0$ , respectively (Nagaraja et al., 2007).

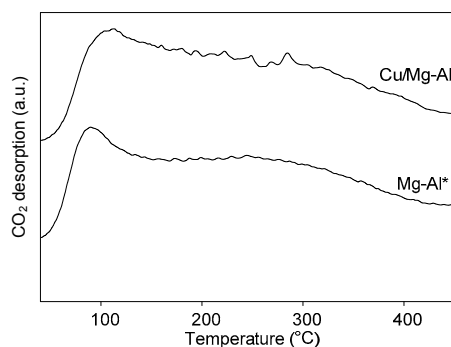


**Fig. 3**  $\text{CO}_2$ -TPD profiles of catalysts

\* Values are obtained from the previous work (Pinthong et al., 2019)

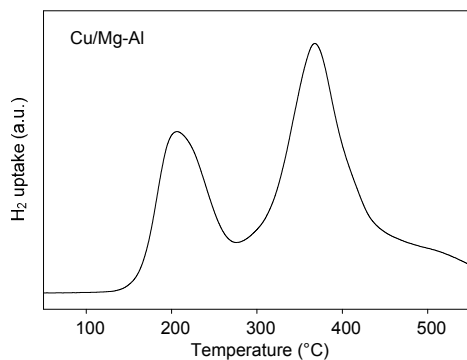


**Fig. 4**  $\text{H}_2$ -TPR profile of Cu/Mg-Al catalyst

## 3.2 Reaction test

### 3.2.1 Effect of copper on the catalytic activity

We investigated the catalytic activity of the Cu/Mg-Al using the oxidative dehydrogenation of ethanol and compared with the performance of the Mg-Al mixed oxide from our previous work (Pinthong et al., 2019). Using the Cu/Mg-Al catalyst, we observed high ethanol conversion in all reaction temperatures. Fig. 5 shows that the ethanol conversion of Cu/Mg-Al extremely increases at  $300^\circ\text{C}$  ( $75.6\%$ ) and slightly increases at the temperature

range of  $300$  to  $400^\circ\text{C}$ . However, at  $400^\circ\text{C}$ , the maximum ethanol conversion of the Cu/Mg-Al catalyst is  $93.0\%$  while that of the Mg-Al catalyst is  $65.3\%$ . In contrast, the acetaldehyde selectivity of Cu/Mg-Al catalyst decreases significantly at  $300^\circ\text{C}$  due to the decomposition of acetaldehyde to carbon dioxide (Fig. 6).

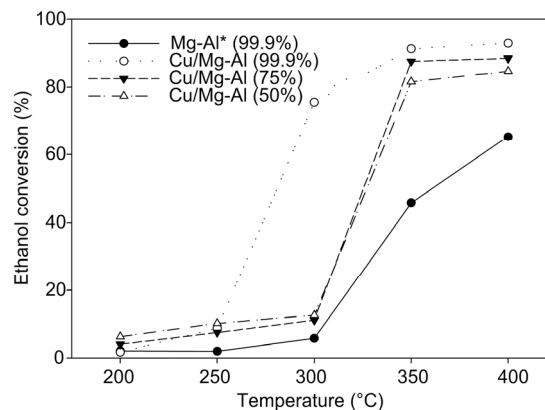


**Fig. 5** Ethanol conversion of the Cu/Mg-Al catalyst under different ethanol concentrations

\* Values of Mg-Al catalyst are obtained from the previous work (Pinthong et al., 2019)

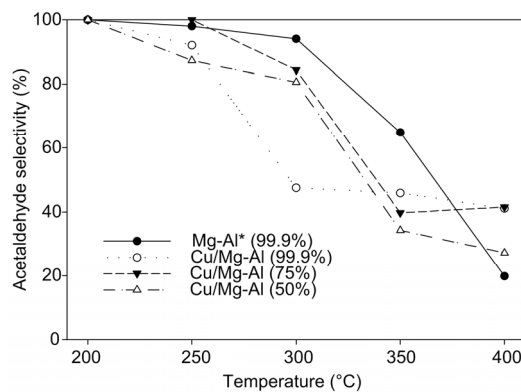


**Fig. 6** Acetaldehyde selectivity of Cu/Mg-Al catalyst under different ethanol concentrations

\* Values of Mg-Al catalyst are obtained from the previous work (Pinthong et al., 2019)

Moreover, we compared the acetaldehyde selectivity of both catalysts at the same ethanol conversion of  $50\%$ . Consequently, we obtained that the acetaldehyde selectivity of the Cu/Mg-Al catalyst was about  $64\%$  at  $280^\circ\text{C}$ . The acetaldehyde selectivity of the Mg-Al catalyst was about  $54\%$  at  $360^\circ\text{C}$ , which was lower than that of Cu/Mg-Al catalyst. Several research shows that the enhancement of the

catalytic activity of the Cu/Mg-Al catalyst is attributed to the copper oxide species on the surface and the base density affects the catalytic performance on the dehydrogenation of ethanol (Janlamool and Jongsomjit, 2017; Quesada et al., 2018).

Fig. 7 shows the proposed mechanism in the presence of the Cu. The reaction starts with the adsorption of the ethanol molecule on the acid/base site of the Mg-Al oxide surface (Idriss and Seebauer, 2000; Andrushkevich et al., 2017). According to research, the ethoxide species are formed through the dissociation of O-H bond of ethanol (Constantino and Pinnavaia, 1995; di Cosimo et al., 1998). The  $\alpha$ -hydrogen is abstracted by CuO to form the acetaldehyde and Cu-O-H group. We observed the desorption of the acetaldehyde molecule, and the O-H group from the Cu surface combines with the H atom from O-H group on the Mg-Al surface to produce water resulting in the Cu<sup>0</sup> formation on the surface. The Cu<sup>0</sup> is consecutively oxidized to CuO by oxygen in the feed (Nair et al., 2011).

### 3.2.2 Effect of ethanol concentration on catalytic activity

In this study, we used different ethanol concentrations as reactants (99.9%, 75%, and 50% by weight in water) in the oxidative dehydrogenation reaction. Fig. 5 shows that at 300 °C, there is a difference in the absolute ethanol conversion and

diluted ethanol conversion. The conversion of the diluted ethanol (75% and 50%) of about 12% was observed. However, this study shows that the presence of water negatively affects the ethanol conversion of the Cu/Mg-Al catalyst. Moreover, Golay et al. (1999) found that there is a high adsorption of water molecules on the active site. At high-temperature range (350–400 °C), the ethanol conversion decreases slightly with the decrease in ethanol concentration. The water content slightly affects the catalytic activity at a high reaction temperature range (Chen et al., 2007). Thus, the Cu/Mg-Al catalyst decreases with increase in reaction temperature. This is due to the water adsorption ability of Cu/Mg-Al catalyst.

Besides, the acetaldehyde selectivity also decreases with an increase in reaction temperature at all conditions (Fig. 6). This is because of the formation of the byproduct such as carbon dioxide, ethylene, diethyl ether, acetic acid, ethyl acetate, 1,3-butadiene, and 1-butanol. However, the Cu/Mg-Al catalyst shows the highest acetaldehyde of 41.8% at 350 °C (Fig. 8). The formation of the carbon dioxide increases with increase in reaction temperature (Fig. 9) due to the complete oxidation of ethanol. This result was evident because of the high ethanol conversion of Cu/Mg-Al. In contrast, the ethylene selectivity increases with the presence of high content of water (low concentration of ethanol) in the feed (Fig. 10).

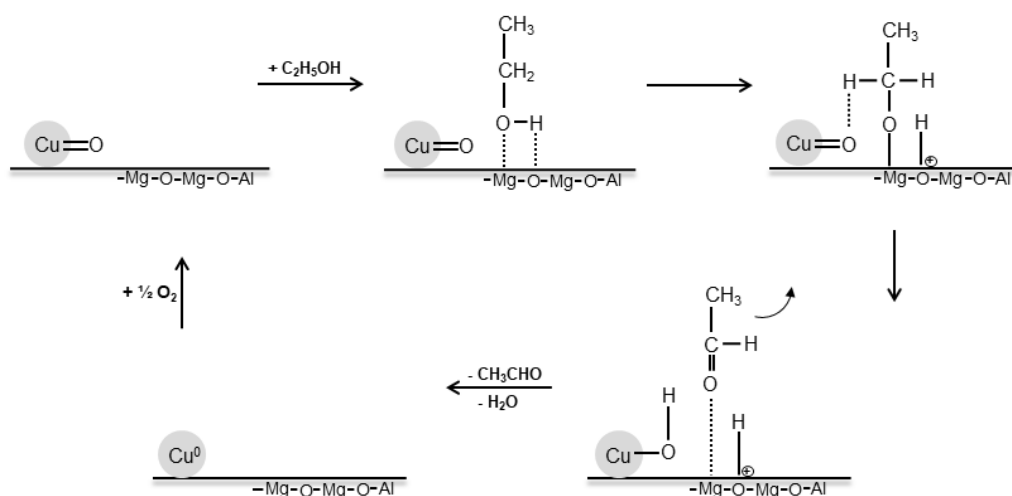
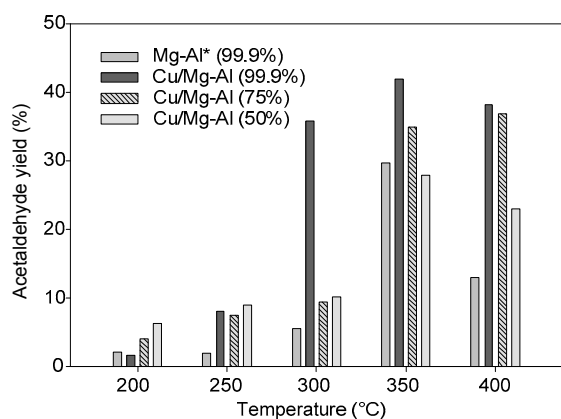


Fig. 7 Proposed mechanism for the oxidative dehydrogenation of ethanol over Cu/Mg-Al catalyst

The increase in the water content of the feed suppresses the catalytic reaction due to the decrease in ethanol conversion (Fig. 5), as a result of the competitive adsorption of water and ethanol on the catalyst surface. Besides, the ethylene selectivity (Fig. 10) increases with the increase of water content in ethanol. This is because the water molecule in the feed reacts with the support (Mg-Al) surface to the form Bronsted acid site, which is very crucial for the ethylene production from ethanol (Golay et al., 1999; Chen et al., 2007). However, the effect of the water content is weak at higher reaction temperature. The carbon dioxide as a byproduct was obtained using Mg-Al at high-temperature range (350–400 °C).



**Fig. 8** Acetaldehyde yield of the Cu/Mg-Al catalyst under different ethanol concentrations

\* Values of Mg-Al catalyst are obtained from the previous work (Pinthong et al., 2019)

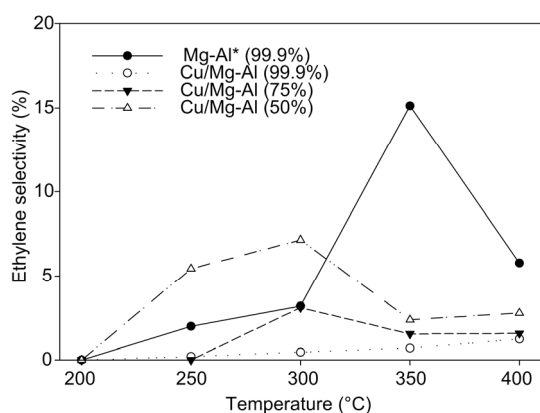


**Fig. 10** Ethylene selectivity of the Cu/Mg-Al catalyst under different ethanol concentrations

\* Values of Mg-Al catalyst are obtained from the previous work (Pinthong et al., 2019)

### 3.2.3 Effect of reduction temperature on catalytic activity

From the proposed mechanism in Fig. 7, the Cu/Mg-Al catalyst is used in the oxidative dehydrogenation of ethanol without reduction step. However, it is reduced by the hydrogen atom from ethanol through the dehydrogenation reaction (Campisano et al., 2018) and re-oxidized to CuO by oxygen in the feed. To support this hypothesis and the results, the effect of the temperature reduction was also investigated (Fig. 11). Finally, we obtained that the ethanol conversion was slightly different with the high-temperature range (350–400 °C). The

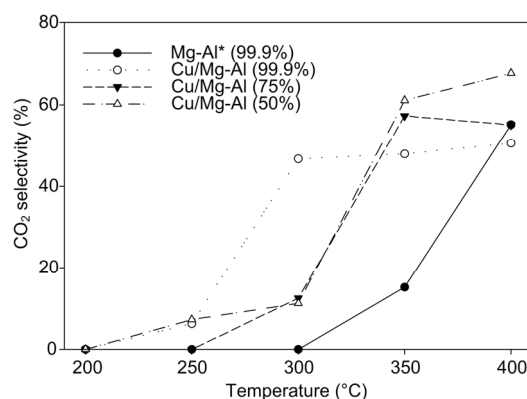


**Fig. 9** Carbon dioxide selectivity of the Cu/Mg-Al catalyst under different ethanol concentrations

\* Values of Mg-Al catalyst are obtained from the previous work (Pinthong et al., 2019)

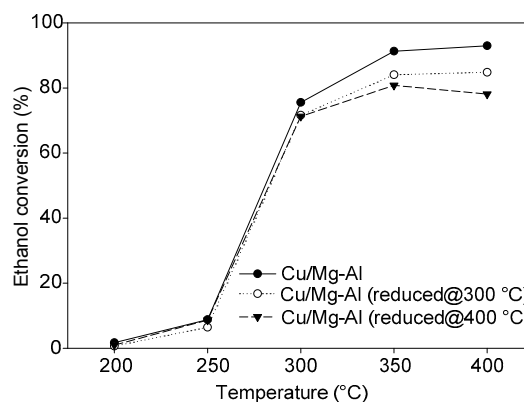


**Fig. 11** Ethanol conversion of the Cu/Mg-Al catalyst under different reduction conditions

non-reduced Cu/Mg-Al catalyst exhibits higher ethanol conversion (5%–10% higher) than the reduced catalysts.

A similar trend was observed in the acetaldehyde selectivity (Fig. 12) and there was a slight difference in the results. The formation of carbon dioxide at high temperatures led to a decrease in acetaldehyde selectivity. Fig. 13 shows the calculation of the acetaldehyde yield of catalysts, indicating that the acetaldehyde yields of reduced catalyst insignificantly differed from non-reduced catalyst. This confirms that the reduction step of the Cu/Mg-Al catalyst is not necessary in the oxidative dehydrogenation reaction of ethanol.

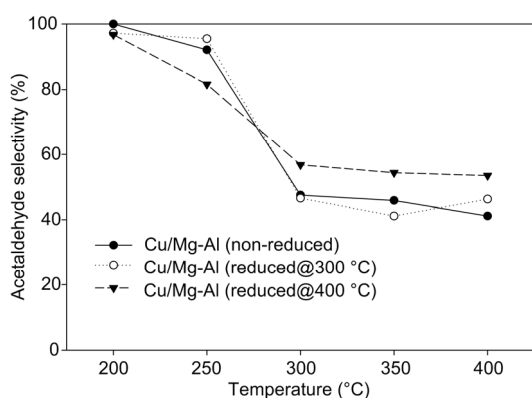


**Fig. 12** Acetaldehyde selectivity of the Cu/Mg-Al catalyst under different reduction conditions

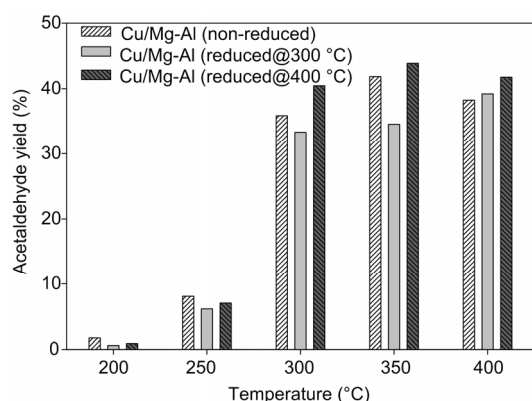


**Fig. 13** Acetaldehyde yield of the Cu/Mg-Al catalyst under different reduction conditions

The stability of the Cu/Mg-Al catalyst was investigated with time-on-stream (TOS) for 10 h. The non-reduced Cu/Mg-Al catalyst was tested in the oxidative dehydrogenation reaction of ethanol

(99.9%) at 350 °C. Here, we obtained the highest acetaldehyde yield. Fig. 14 presents the constant ethanol conversion, showing that the Cu/Mg-Al catalyst was comparatively stable for 10 h. Moreover, to measure the carbon deposition on the spent catalyst from TOS, the thermogravimetric analysis was performed.

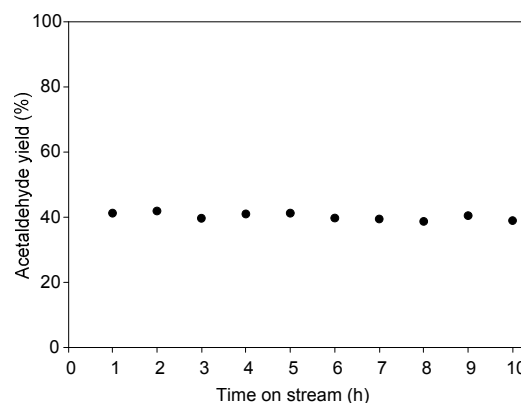


**Fig. 14** Stability test for the Cu/Mg-Al catalyst (without reduction) under the oxidative dehydrogenation of absolute ethanol (99.9%) at 350 °C

Fig. 15 shows the result of the weight loss as a function of temperature. The first region of the weight loss at 200 °C is referred to as the removal of water. Research shows that the weight loss in the temperature range of 200 to 400 °C is attributed to the dehydroxylation and decarbonation of hydrotalcite structure (Yang et al., 2002; Campisano et al., 2018). We calculated the carbon deposition or coke formation on the Cu/Mg-Al catalyst surface in the temperature range of 400 to 800 °C. This is called the de-coking process period (Ahmed et al., 2011). Hence, we obtained that the weight losses of the fresh and spent catalysts in this region were insignificantly different, showing less amount of carbon deposition. The amount of carbon deposition on the spent catalyst was about 2.50%.

Furthermore, we compared the catalytic performance of the Cu/Mg-Al catalyst with other studies. Table 2 shows the acetaldehyde yields of various catalysts. Although the acetaldehyde yield over the Cu/Mg-Al catalyst is not relatively high compared to some catalysts. From our observation, we deduce that the Cu/Mg-Al catalyst is a promising catalyst in the oxidative dehydrogenation of ethanol to acetaldehyde. Hence, we can simply synthesize the

Cu/Mg-Al catalyst by co-precipitation without using severe conditions (e.g. high pressure and temperature) and followed by impregnation. It can be used without any noble metal loading and does not require reduction step before the reaction.

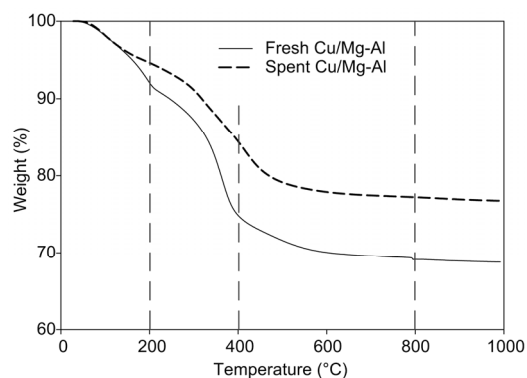


**Fig. 15** Thermogravimetric analysis (TGA) curve of the spent and fresh catalysts

**Table 2** Comparison of the acetaldehyde yield of various catalysts for the oxidative dehydrogenation of ethanol to acetaldehyde

Catalyst	Reaction temperature (°C)	Acetaldehyde yield (%)	Reference
Cu/Mg-Al	350	41.8	This work
Mg-Al-450	350	29.7	Pinthong et al., 2019
AgLi-Al <sub>2</sub> O <sub>3</sub>	225	91	Janlamool and Jongsomjit, 2017
V4b-MCM-41	300	38	Gucbilmez et al., 2006
Au/MgCuCr <sub>2</sub> O <sub>4</sub>	250	95	Liu et al., 2017

## 4 Conclusions

In this study, we investigated the effect of the presence of copper on the performance of the catalyst derived from the Mg-Al hydrotalcite. We prepared the Mg-Al hydrotalcite by co-precipitation followed by calcination, to obtain the mixed oxide. We also prepared the Cu/Mg-Al catalyst by the incipient wetness impregnation of the Mg-Al mixed oxide. From the characterization, we observed that only CuO was present on the surface and the basicity decreases slightly. The activity of the modified catalyst increases remarkably, especially at 300–400 °C. The maximum acetaldehyde yield was 41.8% at

350 °C. Furthermore, the influence of the water content was elucidated by changing the ethanol concentrations in water. The result shows that the water content greatly affects the catalytic performance of the Cu/Mg-Al at 300 °C. We obtained that the ethanol conversion decreases about 6-fold due to the competitive adsorption of the water molecule. However, the negative effect decreases with high reaction temperature (350–400 °C). The effect of the reduction condition was examined by the pre-reducing catalyst at 300 and 400 °C. Thus, we obtained that the reduction step showed an insignificant effect on the catalytic activity of the Cu/Mg-Al. In the TOS study, the catalyst was comparatively stable for 10 h upon TOS test at 350 °C. Hence, we conclude that the Cu/Mg-Al catalyst can be used as a promising catalyst in the oxidative dehydrogenation of ethanol to acetaldehyde without any reduction step. Moreover, it can be used effectively in this reaction for the diluted ethanol at a temperature range of 350–400 °C.

## Contributors

Piriya PINTHONG designed the research and performed the experiment. Bunjerd JONGSOMJIT managed and coordinated responsibility for the research activity planning and execution. Piriya PINTHONG wrote the first draft of the manuscript. Piyasan PRASERTHDAM and Bunjerd JONGSOMJIT helped to organize the manuscript. Piriya PINTHONG and Bunjerd JONGSOMJIT revised and edited the final version.

## Conflict of interest

Piriya PINTHONG, Piyasan PRASERTHDAM, and Bunjerd JONGSOMJIT declare that they have no conflict of interest.

## References

- Ahmed R, Sinnathambi CM, Subbarao D, 2011. Kinetics of de-coking of spent reforming catalyst. *Journal of Applied Sciences*, 11(7):1225-1230. <https://doi.org/10.3923/jas.2011.1225.1230>
- Andrushkevich TV, Kaichev VV, Chesalov YA, et al., 2017. Selective oxidation of ethanol over vanadia-based catalysts: the influence of support material and reaction mechanism. *Catalysis Today*, 279:95-106. <https://doi.org/10.1016/j.cattod.2016.04.042>
- Aramendía MA, Avilés Y, Borau V, et al., 1999. Thermal decomposition of Mg/Al and Mg/Ga layered-double hydroxides: a spectroscopic study. *Journal of Materials Chemistry*, 9(7):1603-1607. <https://doi.org/10.1039/A900535H>

- Blokhina AS, Kurzina IA, Sobolev VI, et al., 2012. Selective oxidation of alcohols over Si<sub>3</sub>N<sub>4</sub>-supported silver catalysts. *Kinetics and Catalysis*, 53(4):477-481.  
<https://doi.org/10.1134/s0023158412040015>
- Campisano ISP, Rodella CB, Sousa ZSB, et al., 2018. Influence of thermal treatment conditions on the characteristics of Cu-based metal oxides derived from hydrotalcite-like compounds and their performance in bio-ethanol dehydrogenation to acetaldehyde. *Catalysis Today*, 306:111-120.  
<https://doi.org/10.1016/j.cattod.2017.03.017>
- Chen GW, Li SL, Jiao FJ, et al., 2007. Catalytic dehydration of bioethanol to ethylene over TiO<sub>2</sub>/γ-Al<sub>2</sub>O<sub>3</sub> catalysts in microchannel reactors. *Catalysis Today*, 125(1-2):111-119.  
<https://doi.org/10.1016/j.cattod.2007.01.071>
- Constantino VRL, Pinnavaia TJ, 1995. Basic properties of Mg<sup>2+</sup><sub>1-x</sub>Al<sup>3+</sup><sub>x</sub> layered double hydroxides intercalated by carbonate, hydroxide, chloride, and sulfate anions. *Inorganic Chemistry*, 34(4):883-892.  
<https://doi.org/10.1021/ic00108a020>
- Dai WL, Cao Y, Ren LP, et al., 2004. Ag-SiO<sub>2</sub>-Al<sub>2</sub>O<sub>3</sub> composite as highly active catalyst for the formation of formaldehyde from the partial oxidation of methanol. *Journal of Catalysis*, 228(1):80-91.  
<https://doi.org/10.1016/j.jcat.2004.08.035>
- di Cosimo JI, Diez V, Xu M, et al., 1998. Structure and surface and catalytic properties of Mg-Al basic oxides. *Journal of Catalysis*, 178(2):499-510.  
<https://doi.org/10.1006/jcat.1998.2161>
- Dias MOS, Modesto M, Ensinas AV, et al., 2011. Improving bioethanol production from sugarcane: evaluation of distillation, thermal integration and cogeneration systems. *Energy*, 36(6):3691-3703.  
<https://doi.org/10.1016/j.energy.2010.09.024>
- Dixit M, Mishra M, Joshi PA, et al., 2013. Physico-chemical and catalytic properties of Mg-Al hydrotalcite and Mg-Al mixed oxide supported copper catalysts. *Journal of Industrial and Engineering Chemistry*, 19(2):458-468.  
<https://doi.org/10.1016/j.jiec.2012.08.028>
- Golay S, Doepper R, Renken A, 1999. Reactor performance enhancement under periodic operation for the ethanol dehydration over γ-alumina, a reaction with a stop-effect. *Chemical Engineering Science*, 54(20):4469-4474.  
[https://doi.org/10.1016/S0009-2509\(99\)00105-0](https://doi.org/10.1016/S0009-2509(99)00105-0)
- Gomez MF, Arrua LA, Abello MC, 1997. Kinetic study of partial oxidation of ethanol over VMgO catalyst. *Industrial & Engineering Chemistry Research*, 36(9):3468-3472.  
<https://doi.org/10.1021/ie970040k>
- Gucbilmez Y, Dogu T, Balci S, 2006. Ethylene and acetaldehyde production by selective oxidation of ethanol using mesoporous V-MCM-41 catalysts. *Industrial & Engineering Chemistry Research*, 45(10):3496-3502.  
<https://doi.org/10.1021/ie050952j>
- Hosoglu F, Faye J, Mareseanu K, et al., 2015. High resolution NMR unraveling Cu substitution of Mg in hydrotalcites-ethanol reactivity. *Applied Catalysis A: General*, 504:533-541.  
<https://doi.org/10.1016/j.apcata.2014.10.005>
- Idriss H, Seebauer EG, 2000. Reactions of ethanol over metal oxides. *Journal of Molecular Catalysis A: Chemical*, 152(1-2):201-212.  
[https://doi.org/10.1016/S1381-1169\(99\)00297-6](https://doi.org/10.1016/S1381-1169(99)00297-6)
- Janlamool J, Jongsomjit B, 2017. Catalytic ethanol dehydration to ethylene over nanocrystalline γ- and γ-Al<sub>2</sub>O<sub>3</sub> catalysts. *Journal of Oleo Science*, 66(9):1029-1039.  
<https://doi.org/10.5650/jos.ess17026>
- Kaneda K, Ueno S, Imanaka T, 1995. Catalysis of transition metal-functionalized hydrotalcites for the Baeyer-Villiger oxidation of ketones in the presence of molecular oxygen and benzaldehyde. *Journal of Molecular Catalysis A: Chemical*, 102(3):135-138.  
[https://doi.org/10.1016/1381-1169\(95\)00055-0](https://doi.org/10.1016/1381-1169(95)00055-0)
- Krutpijit C, Jongsomjit B, 2017. Effect of HCl loading and ethanol concentration over HCl-activated clay catalysts for ethanol dehydration to ethylene. *Journal of Oleo Science*, 66(12):1355-1364.  
<https://doi.org/10.5650/jos.ess17118>
- Kumar S, Gupta R, Kumar G, et al., 2013. Bioethanol production from *Gracilaria verrucosa*, a red alga, in a biorefinery approach. *Bioresource Technology*, 135:150-156.  
<https://doi.org/10.1016/j.biortech.2012.10.120>
- Leofanti G, Padovan M, Tozzola G, et al., 1998. Surface area and pore texture of catalysts. *Catalysis Today*, 41(1-3):207-219.  
[https://doi.org/10.1016/S0920-5861\(98\)00050-9](https://doi.org/10.1016/S0920-5861(98)00050-9)
- Li X, Wang LJ, Xia QB, et al., 2011. Catalytic oxidation of toluene over copper and manganese based catalysts: effect of water vapor. *Catalysis Communications*, 14(1):15-19.  
<https://doi.org/10.1016/j.catcom.2011.07.003>
- Liu P, Li T, Chen HP, et al., 2017. Optimization of Au<sup>0</sup>-Cu<sup>+</sup> synergy in Au/MgCuCr<sub>2</sub>O<sub>4</sub> catalysts for aerobic oxidation of ethanol to acetaldehyde. *Journal of Catalysis*, 347:45-56.  
<https://doi.org/10.1016/j.jcat.2016.11.040>
- Mallat T, Baiker A, 2004. Oxidation of alcohols with molecular oxygen on solid catalysts. *Chemical Reviews*, 104(6):3037-3058.  
<https://doi.org/10.1021/cr0200116>
- Nagaraja BM, Padmasri AH, Seetharamulu P, et al., 2007. A highly active Cu-MgO-Cr<sub>2</sub>O<sub>3</sub> catalyst for simultaneous synthesis of furfuryl alcohol and cyclohexanone by a novel coupling route—combination of furfural hydrogenation and cyclohexanol dehydrogenation. *Journal of Molecular Catalysis A: Chemical*, 278(1-2):29-37.  
<https://doi.org/10.1016/j.molcata.2007.07.045>
- Nair H, Gatt JE, Miller JT, et al., 2011. Mechanistic insights into the formation of acetaldehyde and diethyl ether from ethanol over supported VO<sub>x</sub>, MoO<sub>x</sub>, and WO<sub>x</sub> catalysts. *Journal of Catalysis*, 279(1):144-154.

- <https://doi.org/10.1016/j.jcat.2011.01.011>
- Ob-eye J, Praserttham P, Jongsomjit B, 2019. Dehydrogenation of ethanol to acetaldehyde over different metals supported on carbon catalysts. *Catalysts*, 9(1):66. <https://doi.org/10.3390/catal9010066>
- Papong S, Malakul P, 2010. Life-cycle energy and environmental analysis of bioethanol production from cassava in Thailand. *Bioresource Technology*, 101(S1):S112-S118. <https://doi.org/10.1016/j.biortech.2009.09.006>
- Pinthong P, Praserttham P, Jongsomjit B, 2019. Effect of calcination temperature on Mg-Al layered double hydroxides (LDH) as promising catalysts in oxidative dehydrogenation of ethanol to acetaldehyde. *Journal of Oleo Science*, 68(1):95-102. <https://doi.org/10.5650/jos.ess18177>
- Quaranta NE, Soria J, Corberán VC, et al., 1997. Selective oxidation of ethanol to acetaldehyde on  $V_2O_5/TiO_2/SiO_2$  catalysts. *Journal of Catalysis*, 171(1):1-13. <https://doi.org/10.1006/jcat.1997.1760>
- Quesada J, Faba L, Diaz E, et al., 2018. Copper-basic sites synergic effect on the ethanol dehydrogenation and condensation reactions. *ChemCatChem*, 10(16):3583-3592. <https://doi.org/10.1002/cctc.201800517>
- Ramasamy KK, Gray M, Job H, et al., 2016. Role of calcination temperature on the hydrotalcite derived  $MgO-Al_2O_3$  in converting ethanol to butanol. *Topics in Catalysis*, 59(1):46-54. <https://doi.org/10.1007/s11244-015-0504-8>
- Shan JJ, Janvelyan N, Li H, et al., 2017. Selective non-oxidative dehydrogenation of ethanol to acetaldehyde and hydrogen on highly dilute NiCu alloys. *Applied Catalysis B: Environmental*, 205:541-550. <https://doi.org/10.1016/j.apcatb.2016.12.045>
- Sikander U, Sufian S, Salam MA, 2017. A review of hydrotalcite based catalysts for hydrogen production systems. *International Journal of Hydrogen Energy*, 42(31):19851-19868. <https://doi.org/10.1016/j.ijhydene.2017.06.089>
- Tu YJ, Chen YW, 2001. Effects of alkali metal oxide additives on Cu/SiO<sub>2</sub> catalyst in the dehydrogenation of ethanol. *Industrial & Engineering Chemistry Research*, 40(25):5889-5893. <https://doi.org/10.1021/ie010272q>
- Velu S, Swamy CS, 1996a. Alkylation of phenol with 1-propanol and 2-propanol over catalysts derived from hydrotalcite-like anionic clays. *Catalysis Letters*, 40(3-4):265-272. <https://doi.org/10.1007/BF00815294>
- Velu S, Swamy CS, 1996b. Selective C-alkylation of phenol with methanol over catalysts derived from copper-aluminium hydrotalcite-like compounds. *Applied Catalysis A: General*, 145(1-2):141-153. [https://doi.org/10.1016/0926-860X\(96\)00133-0](https://doi.org/10.1016/0926-860X(96)00133-0)
- Wu L, Zhou T, Cui Q, et al., 2013. The catalytic dehydration of bio-ethanol to ethylene on SAPO-34 catalysts. *Petroleum Science and Technology*, 31(22):2414-2421. <https://doi.org/10.1080/10916466.2011.572102>
- Yang WS, Kim Y, Liu PKT, et al., 2002. A study by in situ techniques of the thermal evolution of the structure of a Mg-Al-CO<sub>3</sub> layered double hydroxide. *Chemical Engineering Science*, 57(15):2945-2953. [https://doi.org/10.1016/S0009-2509\(02\)00185-9](https://doi.org/10.1016/S0009-2509(02)00185-9)

## 中文概要

**题目:** Cu/Mg-Al 水滑石催化剂用于乙醇的氧化脱氢: 乙醇浓度和还原条件的影响

**目的:** 对现有的乙醇氧化脱氢体系中 Mg-Al 催化剂进行改进, 以期获得更高的收率和产物选择性。

**创新点:** 1. 制备 Cu 改性的 Mg-Al 催化剂用于乙醇氧化脱氢反应, 获得了更高的乙醛收率和选择性; 2. Cu/Mg-Al 催化剂制备方法简单, 制备价格低廉 (无需贵金属), 制备条件温和 (无需高温高压); 3. Cu/Mg-Al 催化剂在使用前无需预还原。

**方法:** 1. 采用共沉淀法和浸渍法制备 Cu/Mg-Al 催化剂; 2. 通过乙醇氧化脱氢反应对催化剂进行考评, 以探究 Cu 改性、乙醇浓度和催化剂的还原条件对催化活性的影响。

**结论:** 1. 与 Mg-Al 催化剂相比, 经由 Cu 改性的 Mg-Al 催化剂的乙醇氧化脱氢活性显著提高; 在 350 °C, 乙醛最大收率为 41.8%。2. 进料气中水的存在 (乙醇浓度下降) 会对 Cu/Mg-Al 的催化性能产生不利影响, 使得乙醇转化率和乙醛收率下降; 但在高温区间 (350~400 °C), 这个不利影响有所减弱。3. 反应前, 催化剂在氢气气氛下的还原步骤对 Cu/Mg-Al 催化活性的影响不明显。

**关键词:** 氧化脱氢; 乙醇; 铜; Mg-Al 水滑石; 乙醛; 催化剂